processes

MDPI

Article

Thermogravimetric Study on Peat Catalytic Pyrolysis for Potential Hydrocarbon Generation

Mohammed A. Khelkhal [1,*], Semen E. Lapuk [1], Aleksey V. Buzyurov [1], Tatiana O. Krapivnitskaya [2], Nikolay Yu. Peskov [2], Andrey N. Denisenko [2] and Alexey V. Vakhin [1]

[1] Institute of Geology and Petroleum Technologies, Kazan Federal University, 420008 Kazan, Russia; lapuksemen@gmail.com (S.E.L.); abuzurov95@gmail.com (A.V.B.); vahin-a_v@mail.ru (A.V.V.)
[2] Institute of Applied Physics, Russian Academy of Sciences, 46 Ulyanova St., 603950 Nizhniy Novgorod, Russia; kto465@yandex.ru (T.O.K.); peskov@appl.sci-nnov.ru (N.Y.P.); androu@ipfran.ru (A.N.D.)
* Correspondence: amine.khelkhal@gmail.com; Tel.: +7-(986)-916-39-12

Abstract: Peat has attracted considerable interest as a potential source of alternative fuel in terms of improving hydrocarbons production and satisfying market demand. The next decade is likely to witness a raise in its exploitation. Nevertheless, the characteristics of peat pyrolysis process, via which many experts expect a considerable generation of hydrocarbons, have not been dealt with in depth. In the present study we have applied thermal analysis combined with isoconversional and model methods for clarifying the kinetic and thermodynamic aspects of the process of generating hydrocarbons from peat via pyrolysis in the absence and presence of iron tallates as a catalytic agent. The obtained results showed a positive effect of the opted catalyst on the process of peat pyrolysis. It has been shown that the catalyst is able to reduce the energy of activation of peat pyrolysis process. Moreover, the Gibbs energy, enthalpy and entropy of complex formation values have been found lower in the presence of iron tallates for all the applied isoconversional methods (Friedman and KAS). The evidence from the present study points toward the beneficial effect generated from the utilization of iron tallates in the processes of hydrocarbons generation from peat for improving energy production in the future.

Keywords: peat; TG; Friedman; KAS; catalysis; transition metals; activation energy; enthalpy; entropy; Gibbs free energy

Citation: Khelkhal, M.A.; Lapuk, S.E.; Buzyurov, A.V.; Krapivnitskaya, T.O.; Peskov, N.Y.; Denisenko, A.N.; Vakhin, A.V. Thermogravimetric Study on Peat Catalytic Pyrolysis for Potential Hydrocarbon Generation. *Processes* **2022**, *10*, 974. https://doi.org/10.3390/pr10050974

Academic Editor: Aneta Magdziarz

Received: 25 April 2022
Accepted: 9 May 2022
Published: 13 May 2022

1. Introduction

For the past ten years, there has been a rapid rise in the use of conventional sources for generating more energy in order to satisfy the market demand [1]. However, these sources are likely to witness a considerable decrease due to the political, social and economic situation facing the modern world and community. Scientists generally use the term conventional sources of energy for coal, petroleum, natural gas and nuclear energy. Conversely, the unconventional sources generally include wind, tidal, solar, nuclear and geothermal sources in addition to other sources such as peat [2–4]. A growing body of literature has studied the potential amount of hydrocarbons which could be obtained from peat processing [5–10]. Moreover, the protection of environment is the main subject of research, especially when it comes to the exploitation of fossil fuels. The utilization of fossil fuels contributes to increase CO_2 emission by 78% of the total greenhouse emission since 1970 [11]. In order to face the issues resulted from fossil fuels' uses and to protect the environment, renewable energy sources such as peat are of special importance [12–15]. It is well known that peat differs by the chemical composition and complex nature of its components depending on its source. Although researchers have widely showed interest in peat exploitation, there is still much work to be performed regarding the mechanism of

energy transfer from these sources of energy. Tons of peat is produced annually from different marine and urban solid wastes; agriculture and forests are decaying due to a poorly studied mechanism, resulting in environmental problems and toxic gas emissions [16–19]. Peat is used in different sectors such as medium scale combined heat and power plants, which generate electricity and heat for industrial processes [20]. Moreover, peat represents a potential source of hydrocarbons that can be extracted by applying enhancing oil recovery methods. Enhancing oil recovery (EOR) methods are attracting considerable interest in the petroleum scientific community, which investigates the different sources of energy exploitation. In fact, EOR consist of a set of methods that could be applied for recovering heavy oils and hydrocarbons [21]. EOR is classified into chemical [22], physical [23] and thermal methods [24], depending on the nature of the applied technique. Among the aforementioned methods, thermal methods are presenting a considerable interest in terms of recovery and economy. Perhaps the most attractive method is pyrolysis. It is based mainly on breaking down heavy molecules of peat into light molecules, which leads to easier hydrocarbons flow. Regardless of the promising perspectives expected from the application of pyrolysis for enhancing hydrocarbons generation in industrial plants from peat, this method still needs assistance for higher extraction yields. This could be attended by the application of catalytic systems which may play an important role in changing the behavior of the peat pyrolysis reactions and even effect their parameters. It is common knowledge that the utilization of agrowastes as a source for catalysts is a potential approach for enhancing the reactions of peat pyrolysis [25–28]. Moreover, in our previous works, we have studied the effect of different oil soluble catalysts [29–32] on heavy oil and peat thermal processing and discovered that the use of catalysts decreases the activation energy of the processes of oxidation and pyrolysis, which increase the reactions rate effectively. Thereby, the present study has adopted thermogravimetry in combination with model and free-model kinetic methods and approaches to investigate the effect generated by iron tallates on peat pyrolysis, which of course allowed to suggest further research in the field of peat exploitation and to indicate the process features and challenges.

2. Experimental Part

2.1. Experiments

2.1.1. Materials

We have used a sample of Greko-Ushakov field peat for investigating the process of pyrolysis. The physical properties of the obtained peat are presented in Table 1. For catalytic experiments, we have synthesized iron tallates by using different organic solvents with a high purity (more than 99.5%) provided by Component Reactiv Company. The associated non-organic salts have been purchased from Sigma-Aldrich.

Table 1. The main components contained in the Greko-Ushakovskoye field peat.

Component Composition of Peat Organic Matter	Mass Fraction in the Composition, %
Cellulose	4–10
Humic acids	15–50
Lignin	5–20
Easily hydrolysable compounds	20–40
Water-soluble substances	1–5

2.1.2. Iron Tallates Preparation

The iron tallates have been obtained following the recommendations reported in [33]. Broadly speaking, the process of obtaining iron tallates is mainly based on using distilled tall oil (DTO) as a ligand forming agent. The obtention of iron tallates occurred firstly by mixing 4 g of NaOH with 28.2 g of DTO at room temperature according to the following reaction:

$$C_{17}H_{33}COOH + NaOH \rightarrow C_{17}H_{33}COONa + H_2O \quad (1)$$

The obtained sodium carboxylates solution (30.4 g) has been reacted with 15.2 g of iron sulfates at 70–80 °C as follows:

$$2C_{17}H_{33}COONa + FeSO_4 \rightarrow (C_{17}H_{33}COO)_2Fe + Na_2SO_4 \quad (2)$$

The catalytic experiments have been performed by using 2 wt % of the opted catalyst in the sample of the investigated peat.

2.1.3. X-ray Diffraction Analysis

The X-ray diffraction analysis was performed by using a Shimadzu XRD-7000S automatic powder diffractometer (Kyoto, Japan) via nickel monochromator with a step of 0.008 nm and 3 s exposure time, in combination with a Bruker D2 PHaser and CuKα radiation with a wavelength of λ = 1.54060 nm.

2.1.4. Scanning Electron Microscopy (SEM) Analysis

SEM analysis was performed by the field-emission scanning electron microscope "Merlin" from Carl Zeiss (Oberkochen, Germany) to study the morphology of iron tallates after destruction at higher temperatures. Microscope observation was proceeded by transforming the studied samples to carbon scotch and loading them in a vacuum chamber. The surface morphology was analyzed on secondary electron mode, with a very high resolution (0.8 nm).

2.1.5. Thermal Analysis

In order to study the peat pyrolysis process via thermogravimetric analysis, we have used a STA 449 F1 Jupiter (Netzsch, Selb, Germany) thermoanalyzer in a temperature range of 30–600 °C at different heating rates (5, 15, 20 °C × min^{-1}) under 50 mL·min^{-1} flow of argon gas. The samples' mass was ~10 mg on average in aluminum crucible. Proteus Analysis 5.2.1 and NETZSCH Kinetics Neo 2.1.2.2 program package have been used for data processing.

It is common knowledge that peat pyrolysis processes include different reactions, such as pyrolysis and thermal cracking. These reactions are quite complicated and their understanding requires the application of sophisticated methods of analysis because of the heterogeneous nature of the included reactants and medium's composition. Consequently, studying the kinetic behavior of peat pyrolysis may allow us a deeper understanding of different phenomena, which may be related to the influence of catalysts on enhancing the reactions' rates and mechanisms. For this reason, the application of non-isothermal kinetic approach coupled with the isoconversional and model approach methods will allow us to determine the effect generated by iron tallates on the process of peat pyrolysis and its mechanism.

2.1.6. Kinetic Theory

The complex nature of peat pyrolysis requires a detailed description of its kinetic, which include conversion degree α, the preexponential factor A, and the apparent activation energy E_α in addition to the reaction model $f(\alpha)$ as the main parameters, which is described as follows:

$$\frac{d\alpha}{dt} = k(T)f(\alpha) = Aexp(-\frac{E_\alpha}{RT})f(\alpha) \quad (3)$$

2.1.7. Isoconversional and Model Approach Kinetic Analysis

Themogravimetric analysis has been applied during the present study in order to determine the kinetic triplet of peat pyrolysis in the presence and absence of iron tallates as a catalytic agent for this process. Thus, in order to be able to find these parameters, we applied the Kissinger–Akahira–Sunose (KAS) [34] and Friedman [35] methods as model-free analyses in order to calculate the associated energy of activation E_α and preexponential factor A.

The Kissinger–Akahir–Sunose (KAS) method is presented by the following equation:

$$\ln\left(-\frac{\beta_i}{{T_{\alpha,i}}^2}\right) = Const - \frac{E_\alpha}{RT_{\alpha,i}} \quad (4)$$

The Friedman method is described as follows:

$$\ln\left(\frac{d\alpha}{dt}\right)_{\alpha,i} = \ln[f(\alpha)A_\alpha] - \frac{E_\alpha}{RT_{\alpha,i}} \quad (5)$$

where i is heating rate and $T_{\alpha,i}$ is the temperature at which conversion degree α is reached under ith heating rate. For any given α, the value of E_α is calculated from the slope of the plot $\ln\left(\frac{d\alpha}{dt}\right)_{\alpha,i}$ against $\frac{1}{RT_{\alpha,i}}$ for Friedman and from the slope of the plot $\ln\left(-\frac{\beta_i}{{T_{\alpha,i}}^2}\right)$ against $\frac{1}{RT_{\alpha,i}}$ for KAS. Moreover, kinetic model and the reaction type were found by applying the model-based analysis which depends mainly on the obtained values of activation energy, pre-exponential factor, reaction order, and rate. These models were optimized utilizing KineticsNeo software (Netzsch). The kinetic models have been found with the lowest number of steps to obtain an acceptable fit and consistent approach with the pyrolysis process of peat in the presence and absence of iron tallates. Table 2 presents the classical solid reaction kinetic description.

Table 2. Models' methods for calculating kinetic parameters.

Model	Equation
Reaction of nth order (Fn)	$f = (1-\alpha)^n$
Two-dimensional phase boundary (R2)	$f = 2(1-\alpha)^{1/2}$
Three-dimensional phase boundary (R3)	$f = 3(1-\alpha)^{2/3}$
N-dimensional nucleation according to Avrami–Erofeev (An)	$f = n\cdot(1-\alpha)\cdot[-ln(1-\alpha)]^{(n-1)/n}$
Expanded Prout–Tompkins equation (Bna)	$f = (1-\alpha)^{\,n}\cdot\alpha^{AutocatOrder}$
The reaction of nth order with m-power autocatalysis by-product (Cnm)	$f = (1-\alpha)^n\cdot(1 + AutocatOrder\cdot\alpha^m)$
Kamal–Sourur equation (KS)	$"Reaction\ rate = A"\cdot(1-\alpha)\hat{}n\cdot [exp(-E/RT) + AutocatOrder\cdot\alpha\hat{}m\cdot exp(-E2/RT)]$

2.2. Discussion

2.2.1. Thermogravimetric Analysis

Thermogravimetric analysis is a reliable approach for studying different processes in heterogeneous medium. Thus, its application with small samples allowed us to obtain accurate data in a rapid and economic way. Changes in peat pyrolysis behavior has been carefully investigated in a temperature range of 30–600 °C at different heating rates (5, 15, 20 °C × min^{-1}) in argon medium. The obtained TG curves are presented in Figure 1.

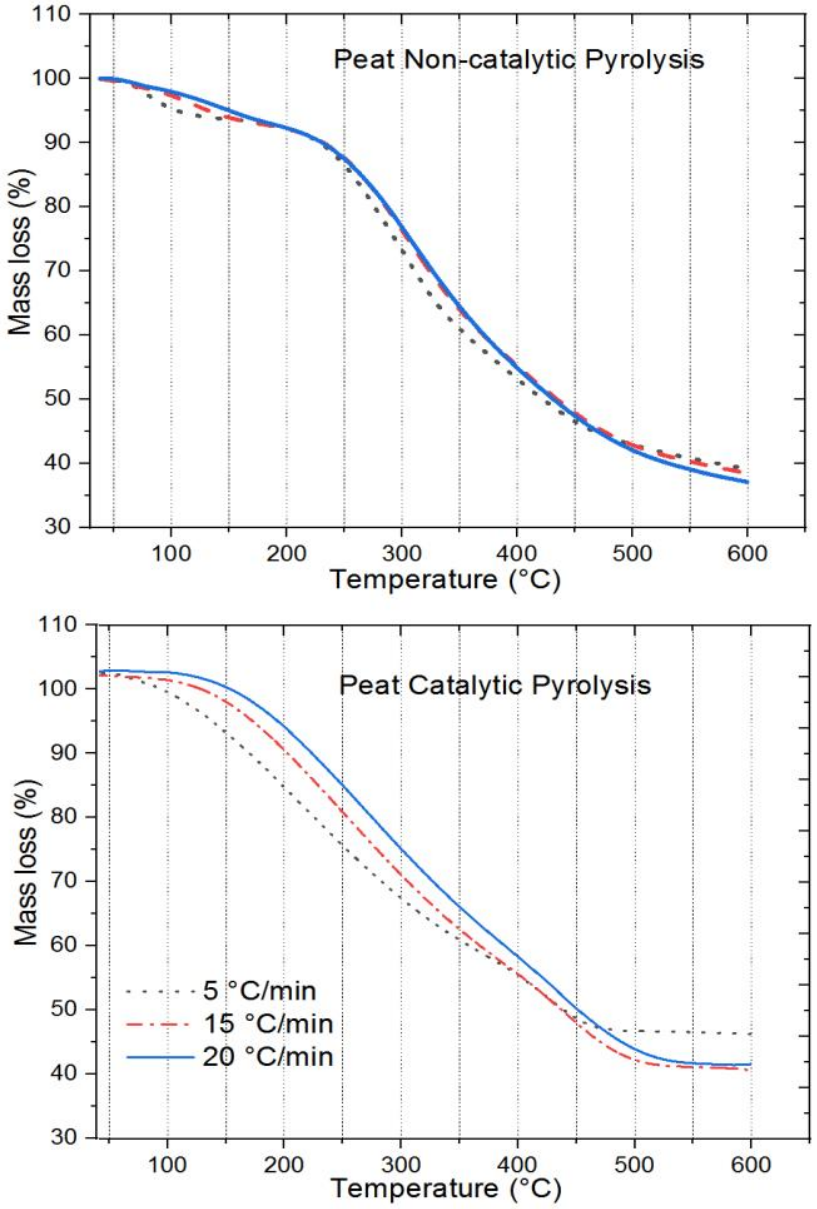

Figure 1. Thermogravimetric curves of the non-catalytic and catalytic processes of peat pyrolysis.

2.2.2. Kinetic Study

In order to emphasize the role played by iron tallates in improving hydrocarbons generation from peat by increasing the pyrolysis reactions' rate, we have applied isoconversional methods together with model approach principle to obtain trustworthy results according to the recommendations provided by the International Confederation for Thermal Analysis and Calorimetry (ICTAC).

Figure 2 and Table 3 present the Friedman and Kissinger–Akahira–Sunose energies of activation of peat pyrolysis in the presence and absence of iron tallates in addition to the associated pre-exponential factors.

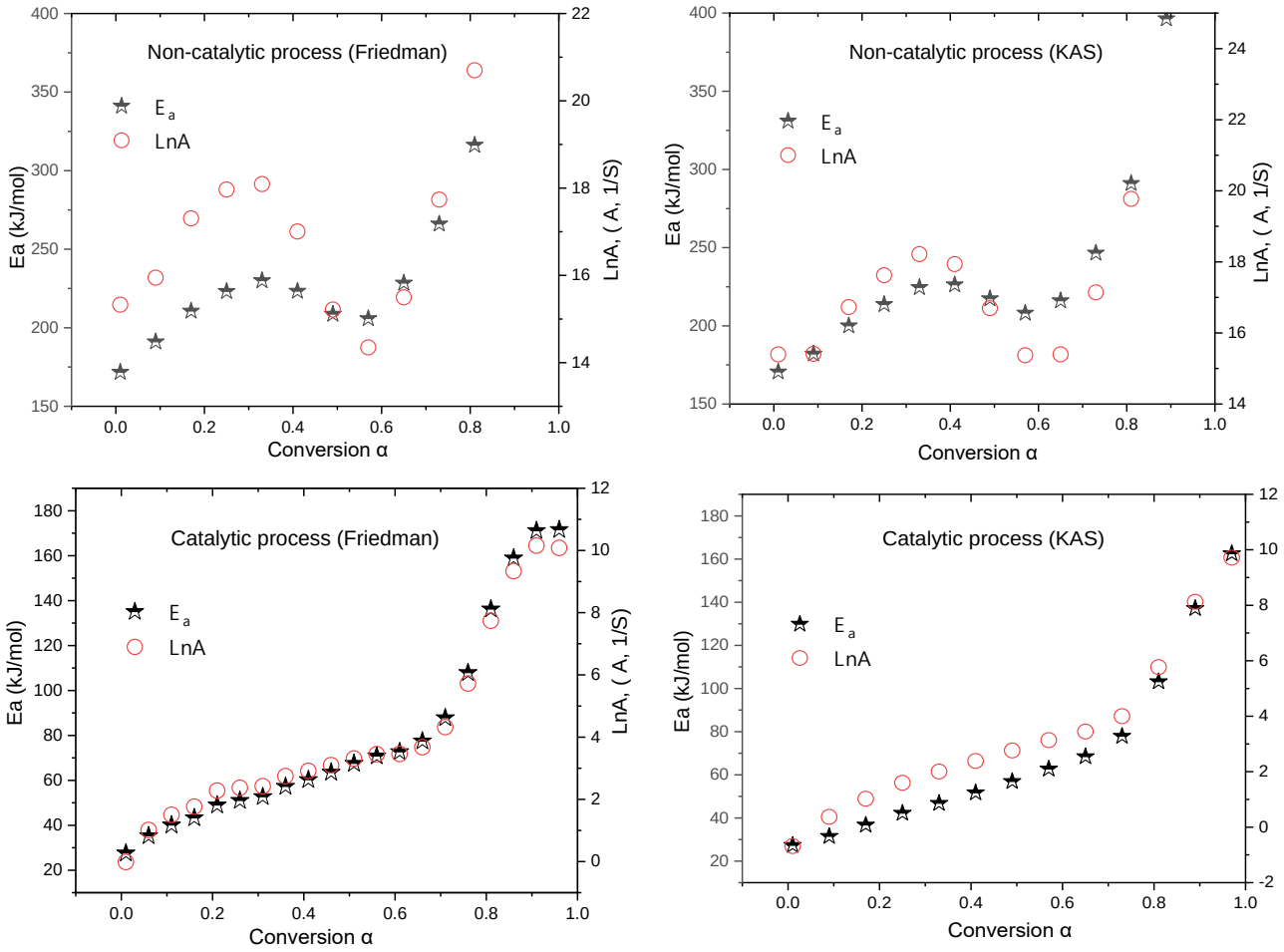

Figure 2. Pyrolysis activation energy and pre-exponential factors dependency on conversion degree in the presence and absence of catalyst obtained by KAS and Friedman.

The obtained curves in Figure 2 demonstrate the multistep nature of peat pyrolysis in the presence and in the absence of iron tallates. In other words, the non-catalytic pyrolysis of peat proceeds through two regions as indicated by the highlighted shoulders of the curve, which demonstrate higher values for both the activation energy at 30% conversion degree and lower values at 60% conversion degree followed by continued increasing until the end of the process. However, introducing iron tallates have completely changed the curves' behavior, where we note a regular increase in the values of activation energy and pre-exponential factors with conversion degree evolution toward the end of the process. We strongly believe that iron tallates have not only decreased the energy of activation of the associated processes, but totally changed the mechanism of peat pyrolysis from a multistep reaction pathway into a para-single one.

It is common knowledge that applying an iso-conversional approach is quite accurate together with the application of model approach. Thereby, we have selected the matching models for the processes of peat pyrolysis in the presence and absence of iron tallates by 16 two-step models for each process of peat pyrolysis. The F-test has been utilized during the process of model selection as recommended by the work provided in [36]. Table 4 highlights the F-test models obtained by a value of 1.000. The values of all parameters are attached to the Supplementary Materials Table S1. Figure 3 presents the TG curves of the obtained peat pyrolysis models in the absence and presence of iron-based catalyst and Table 4 provides the associated parameters to the obtained models.

Table 3. Activation energies of catalytic and non-catalytic pyrolysis process based on KAS and Friedman methods.

	Non-Catalytic Peat Pyrolysis	**Catalytic Peat Pyrolysis**
α/%	$\frac{Ea}{\text{kJ·mol}^{-1}}$	$\frac{Ea}{\text{kJ·mol}^{-1}}$
	Friedman method	
10	194.1 ± 4	39.4 ± 3
20	215.6 ± 0.5	48.4 ± 4
30	228.9 ± 0.7	52.9 ± 4
40	224.8 ± 2.3	59.4 ± 5
50	207.4 ± 0.7	66.9 ± 4
60	211.0 ± 6	72 ± 6
70	251.0 ± 8	84.2 ± 4
80	308.7 ± 1.2	130.4 ± 1.8
90	501.9 ± 66	169.9 ± 2.5
	KAS method	
10	184.5 ± 4	32.3 ± 4
20	205.5 ± 0.8	38.9 ± 5
30	221.2 ± 0.18	45.3 ± 5
40	226.7 ± 2.0	51.1 ± 6
50	215.8 ± 1.4	57.7 ± 6
60	208.1 ± 4	64.7 ± 7
70	233.4 ± 8	72.9 ± 6
80	284.1 ± 1.2	99 ± 4
90	433.8 ± 43	140.9 ± 3

Table 4. Kinetic parameters of peat model pyrolysis processes.

	Peat Catalytic Pyrolysis	**Peat Pyrolysis**
Models	Cnm: E = 39.2 kJ·mole^{-1}, LnA = 1.8 s^{-1}, ReactOrder n = 1.72,	An: E = 153.3 kJ·mole^{-1}, LnA = 12 s^{-1}, Dimension n = 0.5
	Cnm: E = 89.7 kJ·mole^{-1}, LnA = 5.4 s^{-1}, ReactOrder n = 5.76,	Fn: E = 143.2 kJ·mole^{-1}, LnA = 9 s^{-1}, ReactOrder n = 4.54
R^2	0.99961	0.99980
F-test	1.000	1.000

The obtained models have confirmed the aforementioned hypothesis about the behavior of pyrolysis in the presence and absence of iron tallates. In other words, the models obtained for the non-catalytic pyrolysis of peat are associated to two models, which are the An and Fn models, respectively, which witnesses the existence of two main major steps during the reaction mechanism pathway. Unlike non-catalytic process, the models obtained for the catalytic pyrolysis have demonstrated a unique model (Cnm) throughout the whole mechanism pathway, which indicate the para-one step nature of peat pyrolysis in the presence of iron tallates.

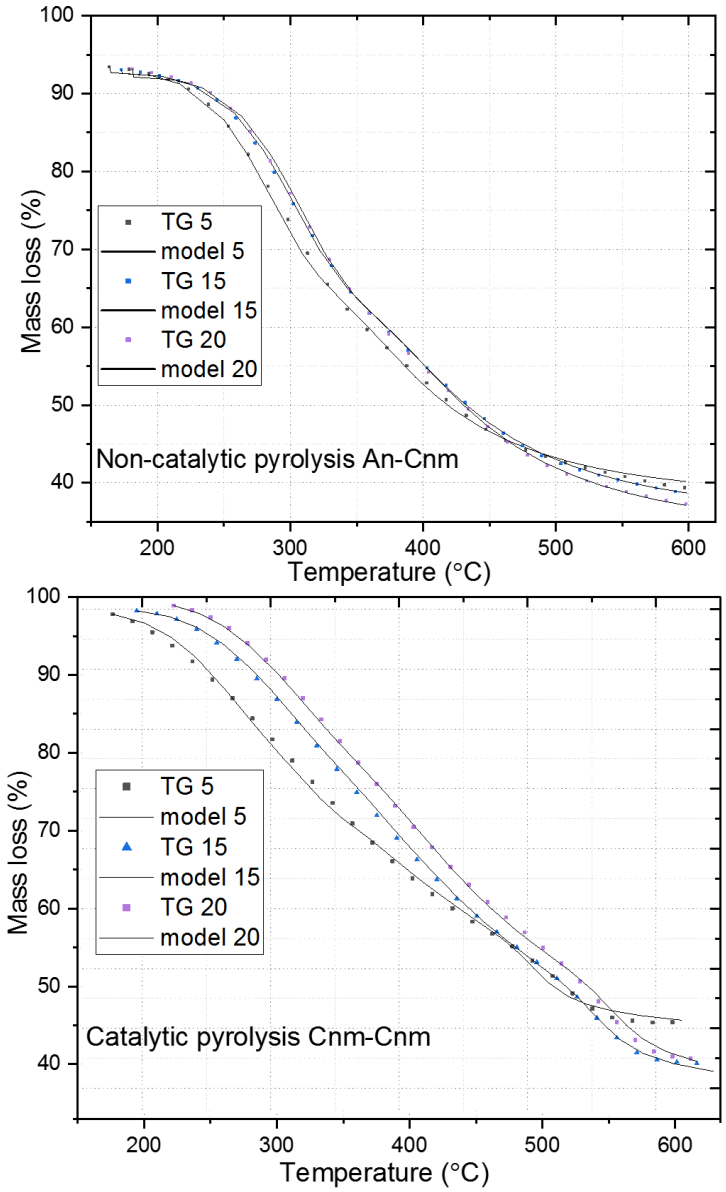

Figure 3. TG model curves of peat pyrolysis in the presence and absence of iron tallates.

2.2.3. Kinetic Predictions

We found much higher values for the preexponential factor in the case of non-catalytic peat pyrolysis process, which in turn may affect the influence provided by the adopted catalyst regardless the fact that it decreases significantly the values of activation energies. Therefore, to confirm the role played by the catalyst, not only in changing the peat pyrolysis mechanism, but in improving the process reaction rate, which, indeed, results in higher yields in shorter time with less energetic loss, we found out the peat conversion time dependency on temperature evolution at different conversion degrees as presented in Figure 4 by taking into consideration 1×10^7 the obtained models in Table 4.

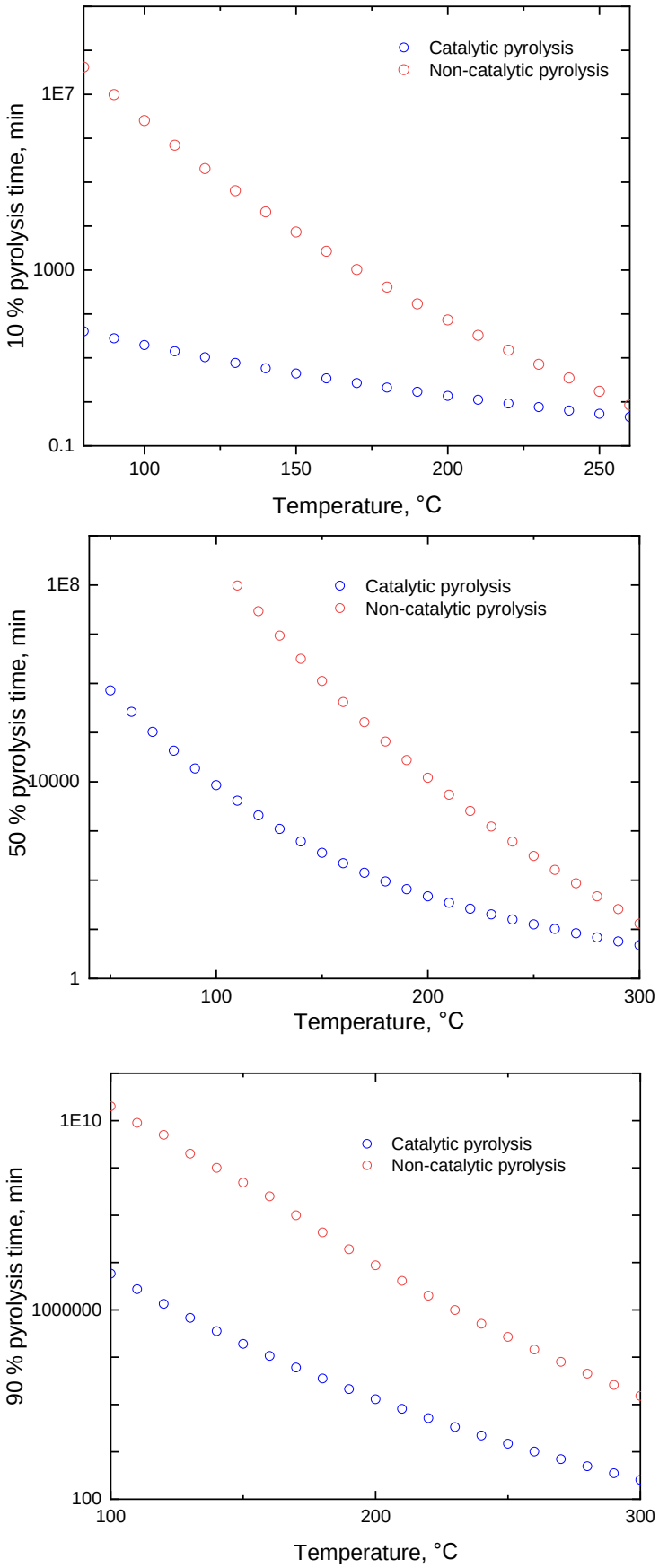

Figure 4. Calculated pyrolysis times of peat in the presence and absence of catalyst at 10%, 50%, and 90% pyrolysis conversions.

The obtained data from Figure 4 indicate the considerable effect generated by iron tallates in enhancing and improving the pyrolysis reactions rate, especially at a temperature range from 200 to 300 °C, which is commonly know as the main zone of high molecular compounds cracking and pyrolysis reactions. In fact, in our previous works [31,37,38], we have proposed the possible mechanism which may occure at this zone in the presence of inert gas such Argon. Our previously published works have confirmed the formation of iron oxide and iron sulfide nanoparticles at this stage (200–300 °C), which mainly catalyze the processes of C-S bonds cleavage on their surfaces. In order to confirm this theory, we have obtained a sample of iron tallates after experiments and applied X-ray diffraction analysis and scanning calorimetric spectroscopy to analyze the obtained nanoparticles. The obtained SEM image and XRD analysis are presented in Figures 5 and 6, respectively.

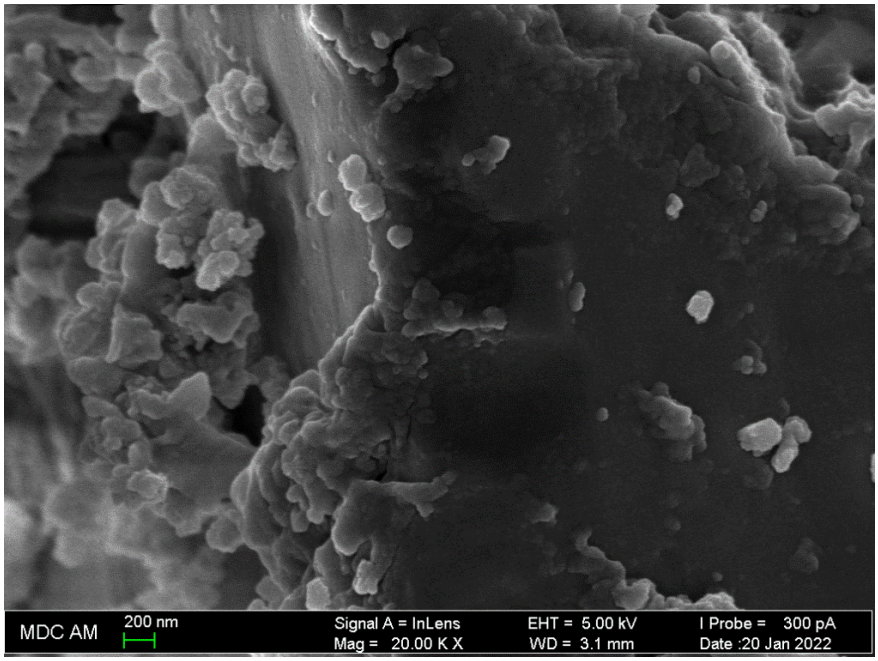

Figure 5. SEM analysis of the obtained catalyst after the pyrolysis process.

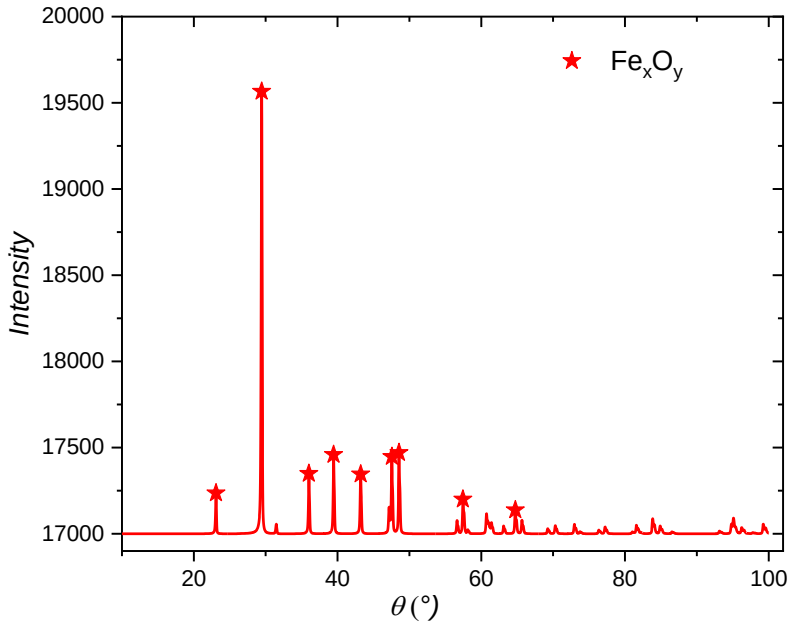

Figure 6. XRD analysis of the obtained catalyst after the pyrolysis process.

As seen from Figures 5 and 6, the iron tallates transforms throughout the pyrolysis process into iron oxide particles of 100–200 nm in average able to catalyze the reactions of cracking and breaking down hetero-carbon bonds at different degrees, which confirm our aforementioned hypothesis about the mechanism of the opted catalyst for the present investigation.

2.2.4. Thermodynamic Functions of Activated Complexes Formation

To further study the peat pyrolysis process, we calculated the thermodynamic functions of the activated complex formation by using the Eyring equation:

$$k(T) = \frac{K_B T}{h} exp\left(-\frac{\Delta^{\ddagger}G^0}{RT}\right) \quad (6)$$

where K_B and h are the Boltzmann and Planck constants and $\Delta^{\ddagger}G^0$ is the standard Gibbs energy of the activation complex formation.

Thus, by assuming that peat pyrolysis is a one-step process at each conversion degree, we would be able to calculate enthalpy $\left(\Delta^{\ddagger}H^0\right)$ and entropy $(\Delta^{\ddagger}S^0)$ changes of the activated complex formation by using the following equations:

$$\Delta^{\ddagger}H^0 = E_{\alpha} - RT_{st} \quad (7)$$

$$\Delta^{\ddagger}S^0 = R\left(ln\frac{hA_{\alpha}}{K_B T_{st}} - 1\right) \quad (8)$$

In Equations (7) and (8) the T_{st} is an arbitrary chosen temperature, which was defined as the peak temperature at the minimum heating rate (473 K)

In order to calculate the standard Gibbs $(\Delta^{\ddagger}G^0)$ energy of the complex formation activation, we have used a well-known equation from the classical thermodynamics course:

$$\Delta^{\ddagger}G^0 = \Delta^{\ddagger}H^0 - T_{st}\Delta^{\ddagger}S^0 \quad (9)$$

The calculated Gibbs energies, enthalpies, and entropies for different conversion degrees were found based on the kinetic parameters obtained from KAS and Friedman methods, and they are presented in Table 5.

The data obtained in Table 5 are illustrated by Figures 7–9.

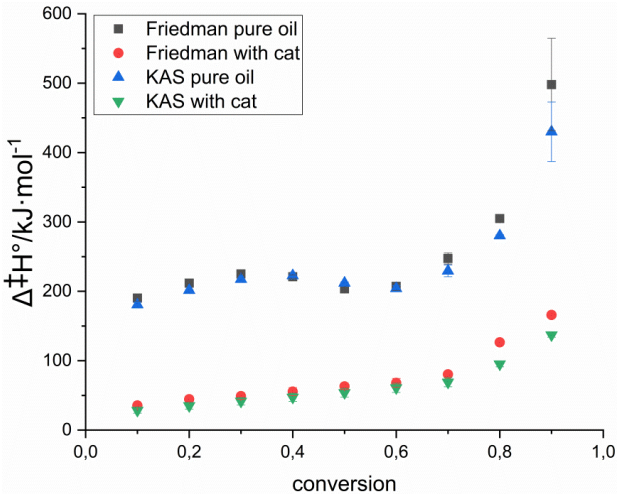

Figure 7. Dependency of the activation enthalpy vs. conversion for catalytic and non-catalytic peat pyrolysis.

Table 5. Activation thermodynamic parameters for catalytic and non-catalytic pyrolysis process based on KAS and Friedman methods.

	Noncatalytic Peat Pyrolysis			Catalytic Peat Pyrolysis		
α/%	$\Delta^{\ddagger}H^{0}$ kJ·mol^{-1}	$\Delta^{\ddagger}S^{0}$ J·mol^{-1}·K^{-1}	$\Delta^{\ddagger}G^{0}$ kJ·mol^{-1}	$\Delta^{\ddagger}H^{0}$ kJ·mol^{-1}	$\Delta^{\ddagger}S^{0}$ J·mol^{-1}·K^{-1}	$\Delta^{\ddagger}G^{0}$ kJ·mol^{-1}
			Friedman method			
10	190 ± 4	52.6 ± 1.0	165 ± 4	36 ± 3	−229.5 ± 0.9	144 ± 3
20	211.8 ± 0.5	79.61 ± 0.11	174.1 ± 0.5	45 ± 5	−214.4 ± 1.2	146 ± 5
30	225.0 ± 0.7	91.08 ± 0.15	182.0 ± 0.7	49 ± 5	−209.8 ± 1.1	148 ± 5
40	220.9 ± 2.3	72.2 ± 0.5	186.8 ± 2.3	56 ± 6	−202.5 ± 1.3	151 ± 6
50	203.5 ± 0.7	30.8 ± 0.15	188.9 ± 0.7	63 ± 5	−194.0 ± 1.0	154 ± 5
60	207 ± 6	21.0 ± 1.2	197 ± 6	68 ± 6	−191.4 ± 1.3	159 ± 6
70	247 ± 8	65.6 ± 1.4	216 ± 8	80 ± 4	−179.2 ± 0.8	165 ± 4
80	304.8 ± 1.2	130.70 ± 0.20	242.9 ± 1.2	126.5 ± 1.8	−116.9 ± 0.3	181.8 ± 1.8
90	498 ± 66	361 ± 11	327 ± 67	166.0 ± 2.5	−64.1 ± 0.4	196.3 ± 2.5
			KAS method			
10	181 ± 4	41.6 ± 1.0	161 ± 4	28 ± 4	−247.9 ± 1.1	146 ± 4
20	201.6 ± 0.8	70.35 ± 0.18	168.3 ± 0.8	35 ± 5	−232.9 ± 1.2	145 ± 5
30	217.35 ± 0.18	88.95 ± 0.04	175.3 ± 0.3	41 ± 5	−221.0 ± 1.3	146 ± 5
40	222.7 ± 2.0	88.1 ± 0.4	181.1 ± 2.1	47 ± 6	−212.3 ± 1.3	148 ± 6
50	212.0 ± 1.4	58.95 ± 0.28	184.1 ± 1.4	54 ± 6	−203.2 ± 1.3	150 ± 6
60	204 ± 4	32.8 ± 0.8	189 ± 4	61 ± 7	−195.0 ± 1.3	153 ± 7
70	230 ± 8	56.2 ± 1.5	203 ± 8	69 ± 6	−186.6 ± 1.2	157 ± 6
80	280.3 ± 1.2	113.59 ± 0.20	226.5 ± 1.2	95 ± 4	−152.3 ± 0.7	167 ± 4
90	430 ± 43	292 ± 7	292 ± 43	137 ± 3	−96.6 ± 0.5	183 ± 3

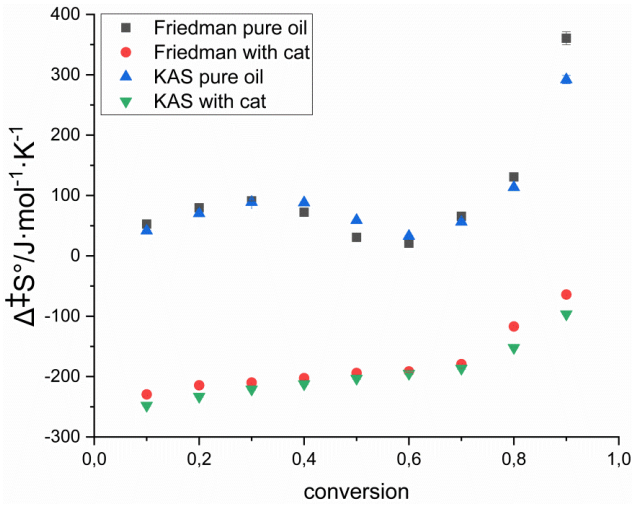

Figure 8. Dependency of the activation entropy vs. conversion for catalytic and non-catalytic peat pyrolysis.

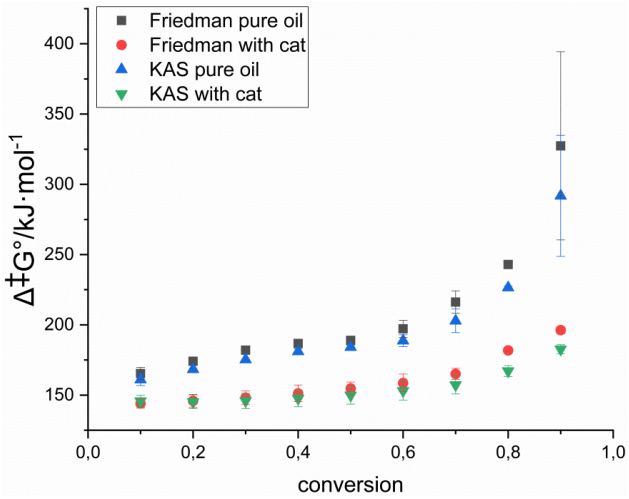

Figure 9. Dependency of the activation Gibbs energy vs. conversion for catalytic and non-catalytic peat pyrolysis.

As can be seen from Figures 7–9, the thermodynamic functions of the activation process calculated based on the data obtained by KAS and Friedman methods are consistent with each other.

Let us begin our discussion with the enthalpy of activation. The dependency of this parameter from conversion degree for non-catalytic decomposition demonstrates three stages. In the first stage, there is an increase ($0.1 \leq \alpha \leq 0.3$), at the second one, there is a decrease ($0.3 \leq \alpha \leq 0.6$), and in the third one ($0.6 \leq \alpha \leq 0.9$), there is a significant increase in activation enthalpy. The reason for this behavior is the multistage characteristic of the pyrolysis process. At the first stage, the cracking of the relatively stable compounds is realized, and less stable compounds are formed. It is supposed that the saturated hydrocarbons of the peat composition, such as easily hydrosable compounds and humic acid, condense at this stage, which leads to the formation of condensed fuel. At the second stage, less stable compounds (the condensed fuel) formed at the first step in addition to cellulose and lignin decompose under thermal cracking reactions, which requires less heat for activation complex formation. At the third stage, the most stable compounds which are presented in coke-like substances undergo decomposition; for this reason, there is a significant increase in the activation enthalpy. For catalytic pyrolysis, the dependence of enthalpy from conversion degree consists of two stages and is located below the non-catalytic curve. Thus, we can conclude that the catalyst significantly reduces the heat required for activation complex formation, and this reduction is more significant for most stable fractions.

The dependences of the activation entropy on the conversion degree are shown in Figure 7. For the case of peat pyrolysis without a catalyst, three stages are observed, and throughout the entire curve, the change in entropy is positive. A positive value of ($\Delta^{\ddagger} S^0$) indicates that the activated complex is more disordered than the initial state. At the same time, when a catalyst is added, the activation entropy has a negative value, which indicates the formation of a more ordered complex. The formation of a more ordered complex leads to a slowdown in the process; however, as will be discussed below, this slowdown is compensated by the enthalpy term.

The results obtained for Gibbs free energy of activation are shown in Figure 9. As is well known, the standard Gibbs energy of the process allows us to estimate the equilibrium constant, which in our case allows us to estimate the amount of the complex being formed. The lower the Gibbs energy is, the greater the amount of the complex is formed, and, therefore, the faster the process will proceed. As can be seen from the analysis of Figure 9, the amount of the activated complex increases with the use of the catalyst, which means that the process will proceed faster.

Thus, from the analysis of Figures 7–9, we can conclude that, in general, the use of iron tallates has a beneficial effect on the rate of the peat pyrolysis process.

3. Conclusions

To sum up, our work has led us to investigate the process of peat pyrolysis in the presence and absence of iron tallates. Moreover, the present work has shed light on the kinetics, thermodynamics and some mechanisms related to peat pyrolysis in the absence and presence of iron-based catalyst. The obtained results showed a positive effect of the opted catalyst on the process of peat pyrolysis. The ability of the used catalyst to transform into nanoparticles, gives it the capacity to change the pyrolysis mechanism from a multistep into a one-step reaction character. Moreover, it has been shown that the catalyst is able to reduce the energy of activation of peat pyrolysis process, which is done by the cracking of C-S, C-O and C-N bonds contained in the peat composition. In addition, the Gibbs energy, enthalpy and entropy of complex formation values have been found to be lower in the presence of iron tallates for all the applied isoconversional methods (Friedman and KAS), which also simplify and increase the reaction rates in the presence of iron tallates. The evidence from the present study points toward the beneficial effect generated from the utilization of iron tallates in the processes of hydrocarbons generation from peat for improving energy production in the future.

Supplementary Materials: The following are available online at https://www.mdpi.com/article/10.3390/pr10050974/s1, Table S1: Kinetic parameters of peat pyrolysis process in the presence and absence of iron tallates obtained by the model approach of non-isothermal kinetics.

Author Contributions: M.A.K.: Formal analysis, Investigation, Writing—original draft, Visualization, Conceptualization. S.E.L.: Formal analysis, Data curation, Visualization. A.V.B.: Formal analysis, Investigation. T.O.K.: Formal analysis, Investigation. N.Y.P.: Formal analysis, Investigation. A.N.D.: Formal analysis, Investigation. A.V.V.: Formal analysis, Investigation, Visualization, Funding acquisition. All authors discussed and approved the final version. All authors have read and agreed to the published version of the manuscript.

Funding: This research received no external funding.

Acknowledgments: This work was supported by the Ministry of Science and Higher Education of the Russian Federation under agreement No. 075-15-2020-931 within the framework of the development program for a world-class Research Center "Efficient development of the global liquid hydrocarbon reserves".

Conflicts of Interest: The authors declare that there is no conflict of interest regarding the publication of this paper.

References

1. Nemati Zadeh Haghighi, A.; Dabiri, A.; Azdarpour, A.; Karaei, M.A. Oxidation Behavior and Kinetics of Iranian Crude Oil Samples Using Thermal Analysis (TA). *Energy Source Part A Recover. Util. Environ. Eff.* **2019**, 1–13. [CrossRef]
2. Suwaid, M.A.; Varfolomeev, M.A.; Al-muntaser, A.A.; Yuan, C.; Starshinova, V.L.; Zinnatullin, A.; Vagizov, F.G.; Rakhmatullin, I.Z.; Emelianov, D.A.; Chemodanov, A.E. In-Situ Catalytic Upgrading of Heavy Oil Using Oil-Soluble Transition Metal-Based Catalysts. *Fuel* **2020**, *281*, 118753. [CrossRef]
3. Omajali, J.B.; Hart, A.; Walker, M.; Wood, J.; Macaskie, L.E. In-Situ Catalytic Upgrading of Heavy Oil Using Dispersed Bio-nanoparticles Supported on Gram-Positive and Gram-Negative Bacteria. *Appl. Catal. B Environ.* **2017**, *203*, 807–819. [CrossRef]
4. Jameel, A.G.A.; Khateeb, A.; Elbaz, A.M.; Emwas, A.-H.; Zhang, W.; Roberts, W.L.; Sarathy, S.M. Characterization of Deasphalted Heavy Fuel Oil Using APPI (+) FT-ICR Mass Spectrometry and NMR Spectroscopy. *Fuel* **2019**, *253*, 950–963. [CrossRef]
5. Wang, L.; Kong, F.; Zheng, M.; Wang, D. Present Situation and Suggestions on the Exploitation and Utilization of Peat Resources in China. *Conserv. Util. Miner. Resour.* **2019**, *39*, 142–147.
6. Waller, M.; Kirby, J. Coastal Peat-beds and Peatlands of the Southern North Sea: Their Past, Present and Future. *Biol. Rev.* **2021**, *96*, 408–432. [CrossRef]
7. Lee, T.; Jung, S.; Hong, J.; Wang, C.-H.; Alessi, D.S.; Lee, S.S.; Park, Y.-K.; Kwon, E.E. Using CO_2 as an Oxidant in the Catalytic Pyrolysis of Peat Moss from the North Polar Region. *Environ. Sci. Technol.* **2020**, *54*, 6329–6343. [CrossRef]
8. Gu, J.; Wang, S.; Lu, T.; Wu, Y.; Yuan, H.; Chen, Y. Synthesis and Evaluation of Pyrolysis Waste Peat Char Supported Catalyst for Steam Reforming of Toluene. *Renew. Energy* **2020**, *160*, 964–973. [CrossRef]

9. Fuchsman, C. *Peat: Industrial Chemistry and Technology*; Elsevier: Amsterdam, The Netherlands, 2012; ISBN 0323157114.
10. Elliott, D.C.; Baker, E.G.; Piskorz, J.; Scott, D.S.; Solantausta, Y. Production of Liquid Hydrocarbon Fuels from Peat. *Energy Fuels* **1988**, *2*, 234–235. [CrossRef]
11. Boden, T.A.; Marland, G.; Andres, R.J. Global, Regional, and National Fossil-Fuel CO_2 Emissions. *Carbon Dioxide Inf. Anal. Center Oak Ridge Natl. Lab. US Dep. Energy Oak Ridge Tenn. USA* **2009**, *10*, 501–510.
12. Weldemichael, Y.; Assefa, G. Assessing the Energy Production and GHG (Greenhouse Gas) Emissions Mitigation Potential of Biomass Resources for Alberta. *J. Clean. Prod.* **2016**, *112*, 4257–4264. [CrossRef]
13. Shuba, E.S.; Kifle, D. Microalgae to Biofuels: 'Promising' Alternative and Renewable Energy, Review. *Renew. Sustain. Energy Rev.* **2018**, *81*, 743–755. [CrossRef]
14. Marsh, G. Biofuels: Aviation Alternative? *Renew. Energy Focus* **2008**, *9*, 48–51. [CrossRef]
15. Yang, Q.Z.; Song, B. Sustainability Assessment of Biofuels as Alternative Energy Resources. In Proceedings of the 2008 IEEE International Conference on Sustainable Energy Technologies, Singapore, 24–27 November 2008; pp. 1001–1006.
16. Lu, Q.; Eid, K.; Li, W.; Abdullah, A.M.; Xu, G.; Varma, R.S. Engineering Graphitic Carbon Nitride (GC_3N_4) for Catalytic Reduction of CO_2 to Fuels and Chemicals: Strategy and Mechanism. *Green Chem.* **2021**, *23*, 5394–5428. [CrossRef]
17. Eid, K.; Lu, Q.; Abdel-Azeim, S.; Soliman, A.; Abdullah, A.M.; Abdelgwad, A.M.; Forbes, R.P.; Ozoemena, K.I.; Varma, R.S.; Shibl, M.F. Highly Exfoliated Ti_3C_2T x MXene Nanosheets Atomically Doped with Cu for Efficient Electrochemical CO_2 Reduction: An Experimental and Theoretical Study. *J. Mater. Chem. A* **2022**, *10*, 1965–1975. [CrossRef]
18. Taherzadeh, M.J.; Karimi, K. Acid-Based Hydrolysis Processes for Ethanol from Lignocellulosic Materials: A Review. *BioResources* **2007**, *2*, 472–499.
19. Taherzadeh, M.J.; Karimi, K. Enzymatic-Based Hydrolysis Processes for Ethanol from Lignocellulosic Materials: A Review. *BioResources* **2007**, *2*, 707–738.
20. Kirkinen, J.; Minkkinen, K.; Penttilä, T.; Kojola, S.; Sievänen, R.; Alm, J.; Saarnio, S.; Silvan, N.; Laine, J.; Savolainen, I. *Greenhouse Impact Due to Different Peat Fuel Utilisation Chains in Finland—A Life-Cycle Approach*; Boreal Environment Research Publishing Board: Helsinki, Finland, 2007.
21. Lake, L.W. *Enhanced Oil Recovery*; Technology & Engineering: Old Tappan, NJ, USA, 1989.
22. Sheng, J.J. *Modern Chemical Enhanced Oil Recovery: Theory and Practice*; Gulf Professional Publishing: Houston, TX, USA, 2010; ISBN 0080961630.
23. Green, D.W.; Willhite, G.P. *Enhanced Oil Recovery*; Henry, L., Ed.; Doherty Memorial Fund of AIME, Society of Petroleum Engineers: Dallas, TX, USA, 1998; Volume 6.
24. Mokheimer, E.M.A.; Hamdy, M.; Abubakar, Z.; Shakeel, M.R.; Habib, M.A.; Mahmoud, M. A Comprehensive Review of Thermal Enhanced Oil Recovery: Techniques Evaluation. *J. Energy Resour. Technol.* **2019**, *141*, 30801. [CrossRef]
25. Eid, K.; Sliem, M.H.; Jlassi, K.; Eldesoky, A.S.; Abdo, G.G.; Al-Qaradawi, S.Y.; Sharaf, M.A.; Abdullah, A.M.; Elzatahry, A.A. Precise Fabrication of Porous One-Dimensional GC3N4 Nanotubes Doped with Pd and Cu Atoms for Efficient CO Oxidation and CO_2 Reduction. *Inorg. Chem. Commun.* **2019**, *107*, 107460. [CrossRef]
26. Gamal, A.; Eid, K.; Abdullah, A.M. Engineering of Pt-Based Nanostructures for Efficient Dry (CO2) Reforming: Strategy and Mechanism for Rich-Hydrogen Production. *Int. J. Hydrog. Energy* **2021**, *47*, 5901–5928. [CrossRef]
27. Gamal, A.; Eid, K.; El-Naas, M.H.; Kumar, D.; Kumar, A. Catalytic Methane Decomposition to Carbon Nanostructures and COx-Free Hydrogen: A Mini-Review. *Nanomaterials* **2021**, *11*, 1226. [CrossRef] [PubMed]
28. Abdu, H.I.; Eid, K.; Abdullah, A.M.; Lu, X. Data on the Synthesis and Characterizations of Carboxylated Carbon-Based Catalyst from Eucalyptus as Efficient and Reusable Catalysts for Hydrolysis of Eucalyptus. *Data Br.* **2020**, *30*, 105520. [CrossRef] [PubMed]
29. Mukhamatdinov, I.I.; Salih, I.S.S.; Khelkhal, M.A.; Vakhin, A. V Application of Aromatic and Industrial Solvents for Enhancing Heavy Oil Recovery from the Ashalcha Field. *Energy Fuels* **2020**, *35*, 374–385. [CrossRef]
30. Vakhin, A.V.; Khelkhal, M.A.; Tajik, A.; Gafurov, M.R.; Morozov, O.G.; Nasybullin, A.R.; Karandashov, S.A.; Ponomarev, A.A.; Krapivnitskaia, T.O.; Glyavin, M.Y. The Role of Nanodispersed Catalysts in Microwave Application during the Development of Unconventional Hydrocarbon Reserves: A Review of Potential Applications. *Processes* **2021**, *9*, 420. [CrossRef]
31. Khelkhal, M.A.; Eskin, A.A.; Nurgaliev, D.K.; Vakhin, A.V. Thermal Study on Stabilizing Combustion Front via Bimetallic Mn@Cu Tallates during Heavy Oil Oxidation. *Energy fuels* **2019**, *34*, 5121–5127. [CrossRef]
32. Khelkhal, M.A.; Eskin, A.A.; Vakhin, A.V. Kinetic Study on Heavy Oil Oxidation by Copper Tallates. *Energy Fuels* **2019**, *33*, 12690–12695. [CrossRef]
33. Feoktistov, D.A.; Kayukova, G.P.; Vakhin, A.V.; Sitnov, S.A. Catalytic Aquathermolysis of High-Viscosity Oil Using Iron, Cobalt, and Copper Tallates. *Chem. Technol. Fuels Oils* **2018**, *53*, 905–912. [CrossRef]
34. Vyazovkin, S. *Isoconversional Kinetics of Thermally Stimulated Processes*; Springer: Berlin/Heidelberg, Germany, 2015; ISBN 9783319141756.
35. Friedman, H.L. Kinetics of Thermal Degradation of Char-forming Plastics from Thermogravimetry. Application to a Phenolic Plastic. *J. Polym. Sci. Part C Polym. Symp.* **1964**, *6*, 183–195. [CrossRef]
36. Freund, J.E.; Perles, B.M. *Modern Elementary Statistics*; Pearson College Division: Upper Saddle River, NJ, USA, 2007.

37. Khelkhal, M.A.; Eskin, A.A.; Sharifullin, A.V.; Vakhin, A.V. Differential Scanning Calorimetric Study of Heavy Oil Catalytic Oxidation in the Presence of Manganese Tallates. *Pet. Sci. Technol.* **2019**, *37*, 1194–1200. [CrossRef]
38. Sitnov, S.; Mukhamatdinov, I.; Aliev, F.; Khelkhal, M.A.; Slavkina, O.; Bugaev, K. Heavy Oil Aquathermolysis in the Presence of Rock-Forming Minerals and Iron Oxide (II, III) Nanoparticles. *Pet. Sci. Technol.* **2020**, *38*, 574–579. [CrossRef]